Epidemics 4 (2012) 33–42

Contents lists available at SciVerse ScienceDirect

Epidemics

journal homepage: www.elsevier.com/locate/epidemics

The role of aquatic reservoir fluctuations in long-term cholera patterns

L. Righetto[a,*], R. Casagrandi[b], E. Bertuzzo[a], L. Mari[a], M. Gatto[b], I. Rodriguez-Iturbe[c], A. Rinaldo[a,d]

[a] Laboratory of Ecohydrology ECHO/IIE/ENAC, Ecole Polytechnique Fédérale Lausanne, Lausanne, Switzerland
[b] Dipartimento di Elettronica e Informazione, Politecnico di Milano, Italy
[c] Department of Civil and Environmental Engineering, Princeton University, Princeton, NJ, USA
[d] Dipartimento IMAGE & International Center for Hydrology, "Dino Tonini", Università di Padova, Padova, Italy

ARTICLE INFO

Article history:
Received 24 May 2011
Received in revised form
19 September 2011
Accepted 20 November 2011
Available online 6 December 2011

Keywords:
Waterborne diseases
Seasonally forced model
Chaotic time-series
Hydrologic seasonality and cholera

ABSTRACT

We propose and analyze an important extension of standard cholera epidemiological models, explicitly accounting for fluctuations of water availability to the human community under study. The seasonality of water input in the reservoir drives the variation of concentration of *Vibrio cholerae*. Two compartments are added to the Susceptible-Infected-Bacteria model. First, the recovered individuals, which, over many seasons, lose their immunity to the disease and replenish the Susceptible group. Second, the water volume of the reservoir, which determines bacterial dilution and, consequently, the probability of contracting cholera by ingesting contaminated water. By forcing the model with a seasonally varying hydrologic input, we obtain simulations that can be compared to available data for various regions of the World characterized by different hydrological and epidemiological regimes. The model is shown to satisfactorily reproduce important characteristics of disease insurgence and long-term persistence. Using bifurcation analysis of nonlinear systems, we also explore how different degrees of seasonality and values of the basic reproductive number can change the expected long-term epidemiological time series. We find that there exist parametric conditions where the model shows chaotic patterns – i.e. high unpredictability especially in the amplitude of prevalence peaks – which very much resemble actual data on long-term cholera insurgence.

Introduction

Cholera is an intestinal disease that can cause death of the host by dehydration due to profuse diarrhoea and vomiting. As the recent and violent Haiti epidemics testifies (Bertuzzo et al., 2011; PAHO, 2011; Tuite et al., 2011), cholera outbreaks can be a major threat for developing countries. In this context, mathematical modelling is becoming a subject of increasing epidemiological interest (Tuite et al., 2011; Bertuzzo et al., 2008; Mari et al., 2012; Chao et al., 2011), both for acute epidemics, which tend to have self-sustained dynamics driven by exposure to excess concentrations of pathogens through dispersal by water pathways and human mobility, and for recurrent events in endemic regions, i.e. outbreaks due to hydrometeorological seasonality and to the ecology of the *Vibrio cholerae*. In particular, research is needed to better understand the mechanisms of its recurring insurgence in endemic regions, i.e. where outbreaks of the disease are cyclically observed. The role of many environmental drivers has been examined to date (see e.g. Akanda et al., 2009; Colwell, 1996; Pascual et al., 2002), but there is no clear indication of a robust, unambiguous correlation between one exogenous forcing factor and long-term cholera patterns. Viability of *V. cholerae* in riverine and marine environments is obviously a key factor, which depends on many hydroclimatological variables, such as water temperature and precipitation or flooding indices as symptoms of increased exposures (Pascual et al., 2002; Bouma and Pascual, 2001; Altizer et al., 2006; Ruiz-Moreno et al., 2007). On the other hand, bacterial concentration in the local water reservoir, i.e. in the water volume that is commonly utilized by the local community for its daily needs, is directly related to the hydrological cycle. The dilution effect is the expected mechanism underlying the link between the seasonal fluctuations of water reservoir volumes and the insurgence of the disease – the intensity of droughts has, in fact, been found to be positively correlated with the intensity of the disease Akanda et al. (2009). Our aim is to systematically analyze via a newly proposed model the influence of different hydrological regimes on cholera long-term temporal patterns to understand whether this factor has indeed a key role in determining the observed periodicities and bursts of the disease in various geographic regions.

To focus on temporal fluctuations, we will use a spatially implicit description and discuss the different epidemiological patterns that can affect a single human community as a result of time-varying water availability. We thus assume that the time scale of spatial spread of the disease in the whole region considered (through

* Corresponding author.
E-mail address: lorenzo.righetto@epfl.ch (L. Righetto).

1755-4365/$ – see front matter © 2011 Elsevier B.V. All rights reserved.
doi:10.1016/j.epidem.2011.11.002

dispersion in waterways and human mobility) is much shorter than the time scale of the local epidemics (see Bertuzzo et al., 2010 for details). Under this circumstance, spatially explicit and spatially implicit models basically show a very similar behavior, as individuals move rapidly inside the region without introducing large delays at the epidemic time scale. Spatially detailed models relating transport of bacteria along river networks and cholera insurgence were previously addressed in the literature (Bertuzzo et al., 2010, 2008; Righetto et al., 2011; Tuite et al., 2011; Chao et al., 2011), but the seasonal variations of water volumes in the river network were not considered therein. This is a factor that needs to be addressed, because there is ample evidence that the variable conditions of water supply are tightly linked to cholera temporal patterns (Akanda et al., 2009).

The core of our model is based on Codeco's Susceptible-Infected-Bacteria (SIB) compartmental model Codeco (2001), suitably modified to explicitly incorporate temporary immunity of hosts and the water reservoir dynamics. In the original formulation of Codeco (2001) the host population was subdivided into susceptible and infected compartments alone. The disease was indirectly transmitted via ingestion of water contaminated by *V. cholerae*. Because we want to study long-term (i.e. several years) cholera patterns, we need to account for the process of immunity loss by individuals who recovered from the disease. We therefore add a third compartment in the population. Also, as first proposed by Pascual et al. (2002), here we consider the variation over time of the volume of water available to the community, expressed as a mass balance equation. The amount of water available in the system influences in a nonlinear way not only the concentration of bacteria, but also the probability of contracting the disease.

We specifically aim at investigating the role played by hydrological seasonality in the processes leading to cholera insurgence. We do not restrict our focus only to areas of historically acknowledged endemicity of the disease (Pascual et al., 2002, 2000), but we extend the analysis to countries with sporadic cholera outbursts to understand whether hydrological seasonality alone can reproduce – at least qualitatively – some of the global patterns that have been identified at different latitudes (Lipp et al., 2002; Emch et al., 2008).

To investigate which causal factors are key for the insurgence of various epidemiological patterns, we use bifurcation analysis of nonlinear systems (Kuznetsov, 1995). To this end, in fact, it is the most effective tool, because it permits to systematically classify the different possible behaviors of the model and to link them to particular model parameterizations. Since the majority of model parameters can be given reliable estimates from the literature (Codeco, 2001; Hartley et al., 2006; Neilan et al., 2010) and do not display very pronounced geographical variations, we concentrate here on a few, significant quantities that are either characterized by uncertainty or do vary appreciably in different regions of the world. In particular, we have singled out the basic reproductive number R_0, the variability of the hydrological cycle (also called degree of seasonality) and the water reservoir residence time. Lastly, we have tested how different dynamics of loss of immunity, whose duration has also been questioned (see King et al., 2008), may affect the behavior of the model.

The paper is organized as follows. 'The model' section introduces the model which includes the dynamics of the local reservoir of water. In the 'Epidemiological patterns originated by the model' section, we exemplify the temporal patterns of the forced behavior produced by the model for a set of parameter values and compare model outputs with data observations. In the 'Bifurcation analysis of the model' section we completely analyze the patterns of model behaviors as a function of the focal parameters via bifurcation analysis. A discussion and some final remarks close the paper ('Conclusions' section).

The model

To analyze the role played by the dynamics of the water reservoir in determining the epidemiology of cholera, we reformulate the basic model by Codeco (2001) as follows:

$$\begin{aligned}
\frac{dS}{dt} &= \mu(H-S) - \beta\frac{B}{kW+B}S + \rho R \\
\frac{dI}{dt} &= \beta\frac{B}{kW+B}S - (\mu+\alpha+\gamma)I \\
\frac{dR}{dt} &= \gamma I - (\rho+\mu)R \\
\frac{dB}{dt} &= -\mu_B B + pI - \lambda B \\
\frac{dW}{dt} &= q(t) - \lambda W
\end{aligned} \tag{1}$$

where S, I and R are respectively the number of susceptible, infected and recovered individuals in the host community of size H; B is the total number of *V. cholerae* bacteria, contained in the water reservoir of size W (thus bacterial concentration is B/W). The human population is assumed to be at demographic equilibrium in the absence of cholera, with μ being the natural background mortality rate and H the demographic equilibrium. Infection is regulated by the contact rate β and depends on the number of bacteria B through the logistic dose–response curve introduced by Codeco (2001), i.e. $B/(kW+B)$; the parameter k represents the concentration of bacteria that grants 50% probability for a susceptible of contracting the disease. Once infected, individuals can die either from natural causes (μ) or from cholera infection (α), or they can recover from the disease at a rate γ. As for *V. cholerae* dynamics, we assume that bacteria would not persist in the natural environment, at least in appreciable quantities (μ_B being their mortality rate), in the absence of contamination due to faecal excretion by infected individuals (occurring at rate p). We note that I includes asymptomatic individuals as well, whose excretion represents an important input to *V. cholerae* concentration in the water (King et al., 2008).

As anticipated in the 'Introduction' section, we have added two model compartments to the Codeco model Codeco (2001). The first is the recovered class R. Infection from *V. cholerae* does not confer total immunity from cholera. Therefore recovered individuals have an active role in the long-term epidemiology of the disease, because they replenish the susceptible compartment at a rate ρ, which is compatible with the decadal temporal scales of our interest. Most studies indicate in fact a long-lasting immunity of about 5 years (Clemens et al., 1990; Koelle et al., 2005), even though a shorter immunity duration of 12 weeks has been advocated for in other studies (see e.g. King et al., 2008). Second, as suggested in Pascual et al. (2002), we explicitly incorporate a description of the hydrologic dynamics of the water reservoir volume W. The water reservoir receives an input $q(t)$ and it is depleted at a rate λ, which is here assumed to be mainly due to drainage (i.e. evaporation is considered small with compare to drainage). The outflux of water from the water reservoir (λW) determines also an output of *V. cholerae* proportional to the actual concentration B/W. This is indeed the simplest possible hydrologic assumption, not devoid of practical appeal (Brutsaert, 2005). We define the characteristic size of the water reservoir as $\overline{W} = q_0/\lambda$, where q_0 is the time average of $q(t)$ (i.e. $q_0 = 1/T \int_{t_0}^{t_0+T} q(t)\,dt$, for $T \gg 1/\lambda$). The interactions among the model compartments are illustrated in Fig. 1, while a summary of the symbols used for parameters is in Table 1. To mathematically simplify the analysis, the model is reformulated in terms of dimensionless variables, i.e. $S \triangleq (S/H)$, $I \triangleq (I/H)$, $R \triangleq (R/H)$, $W \triangleq (W/\overline{W})$ and $B \triangleq (B/k\overline{W})$.

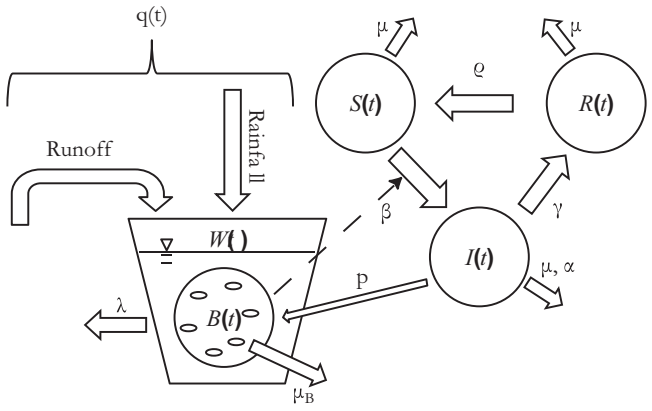

Fig. 1. Schematic graph with the interactions among compartments of model (2) and the basic processes involved in the dynamics of the system.

The rescaled model therefore reads as:

$$\begin{aligned}
\frac{dS}{dt} &= \mu(1-S) - \beta\frac{B}{W+B}S + \rho R \\
\frac{dI}{dt} &= \beta\frac{B}{W+B}S - (\mu+\alpha+\gamma)I \\
\frac{dR}{dt} &= \gamma I - (\rho+\mu)R \\
\frac{dB}{dt} &= -\mu_B B + \frac{pH}{k\overline{W}}I - \lambda B \\
\frac{dW}{dt} &= Q(t) - \lambda W
\end{aligned} \tag{2}$$

where $Q(t) = q(t)/\overline{W}$. Consistently with Codeco (2001), we find that model (2) – when $Q(t)$ is kept constant – has two epidemiological equilibria, namely the disease-free equilibrium $\overline{X}_0 = [1\,0\,0\,0\,1]^T$ (the symbol T stands for matrix transposition) and the non-trivial, endemic equilibrium $\overline{X}_+ = [S_+\, I_+\, R_+\, B_+\, 1]^T$. In particular, X_+ is positive and the model converges to endemicity only when the basic reproductive number of cholera, R_0 (Anderson and May, 1992), i.e.

$$R_0 = \frac{\beta p H/k\overline{W}}{(\mu+\alpha+\gamma)(\mu_B+\lambda)} \tag{3}$$

is larger than unity. It can be shown that at equilibrium the prevalence I_+ (the fraction of infected individuals) increases with R_0. When $R_0 < 1$, $\overline{X}_0$ is stable. Note that, at $R_0 = 1$, there is a so-called transcritical bifurcation of the system: equilibria $\overline{X}_0$ and X_+ coincide and exchange stability (Kuznetsov, 1995).

R_0 is directly proportional to the contact rate β and the excretion rate p, to the total size of the human community H and to the times of residence in the compartments of infectives $(\mu+\alpha+\gamma)^{-1}$ and bacteria $(\mu_B+\lambda)^{-1}$. On the other hand, it is inversely proportional to the critical dose k and to the characteristic water volume $\overline{W}$ (the dilution effect).

Model (2) has 8 parameters, each with a specific epidemiological or hydrological meaning. Ranges for the numerical values of the majority of these parameters can be found in the literature (see Bertuzzo et al., 2008; Codeco, 2001 for references). As for the average transition time from recovered to susceptible state, we assume here that immunity is lost after 5 years (Koelle et al., 2005), so $\rho = 0.00055$ days^{-1}. This assumption will be relaxed in 'Bifurcation analysis of the model' section. Hydrologic parameters will be discussed in the next section.

Table 1
Description of the parameters used in the model.

Symbol	Description
β	Rate of exposure to contaminated water (day^{-1})
μ	Population natality and mortality rate (day^{-1})
p	Per capita contamination rate (cells day^{-1} infected^{-1})
H	Human population size at demographic equilibrium
γ	Recovery rate (day^{-1})
k	Concentration of *V. cholerae* in water that yields 50% chance of being infected with Cholera (cells/m^3)
α	Cholera mortality rate (days^{-1})
μ_B	Natural mortality rate of *V. cholerae* in the aquatic environment (day^{-1})
λ	Rate of drainage from the water reservoir (day^{-1})
ρ	Loss of immunity rate (day^{-1})

Epidemiological patterns originated by the model

As outlined in the 'Introduction' section, our goal is to investigate how epidemiological dynamics are connected to the hydrological regime. To this end we introduce an idealized seasonal pattern for the water input $Q(t)$, which qualitatively mimics the seasonality of river flow and/or rainfall. Such fluctuations represent the typical hydroclimatic conditions of many regions in the world. In formulas, we set:

$$Q = Q_0\left[1 + \epsilon\cos\left(\frac{2\pi t}{365}\right)\right] \tag{4}$$

where Q_0 is the annual average normalized flow and t is measured in days. The parameter ϵ is a measure of the flow variability – the larger is ϵ, the larger is the ratio of the variance to the mean. This simplified formalism corresponds to a unimodal hydrological pattern, characterized by one annual peak occurring in the appropriate season depending on the region. It is worth noting that not all regions of the world have a unimodal precipitation pattern. For instance some regions display bimodal patterns (Ruiz-Moreno et al., 2007).

A first question concerns whether the processes described by the seasonally forced model can reasonably reproduce, at least qualitatively, epidemiological behaviors observed in data. Unfortunately, available studies that point at the role of seasonality in cholera transmission (e.g. Pascual et al., 2002; Lipp et al., 2002; Emch et al., 2008) do not discuss in quantitative detail the interplay between hydrological drivers and cholera insurgence. In a recent and exhaustive review on seasonality of cholera, Emch et al. (2008) show data for the disease in areas of the world at different latitudes. Among many other examples of the same kind, cholera in Iran shows a pattern of insurgence that clearly suggests periodicity, with yearly outbreaks concentrating in October. Rainfall data from the Iran Meteorological Service are available online (Iran Meterological Service, 2011). By aggregating throughout the whole region data from rain gauges for the months between 1973 and 2004, we obtain a clearly unimodal pattern (Fig. 2A, blue bars), with a wet season (late winter/early spring), followed by a dry summer. The red bars in the same Fig. 2A show the sum of cholera outbreaks occurred in Iran month by month between 1974 and 2005, as reported in Emch et al. (2008). Note that an outbreak is defined therein as the presence of at least one reported cholera case in any calendar month, which cannot be referred to as an actual peak of prevalence, but simply testifies the occurrence of cholera in the region during the specific month. Although such an aggregated indicator must not be confused with disease prevalence, it is plausible to consider the number of outbreaks recorded in a month during the study period as a proxy for the infected in that month.

In panel B of Fig. 2 we show the temporal pattern (red solid line) of prevalence predicted after transient by model (2) when forced with a fluctuating water input $Q(t)$, as the light blue solid line. We assume here $\epsilon = 0.7143$, which corresponds approximately to the percent variation from the mean that is observed in rainfall data shown in panel A. For values of R_0 slightly larger than unity (we

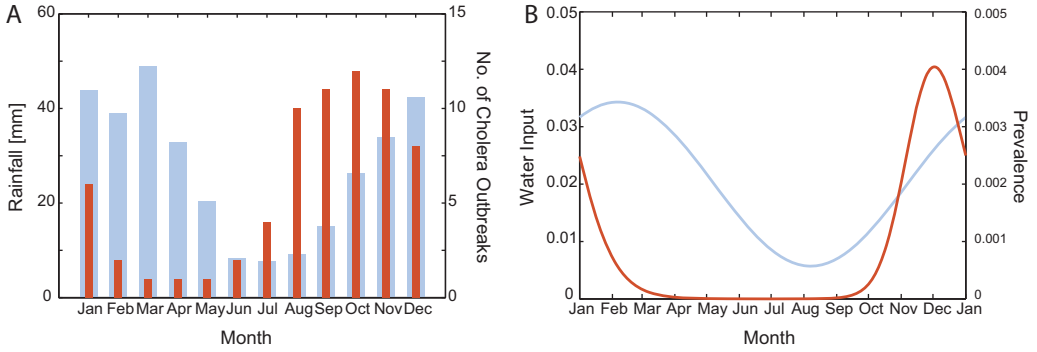

Fig. 2. (A) Data for the annual rainfall regime in Iran (light blue, left axis), obtained aggregating data from the Iran Meterological Service (2011) of Iranian stations (monthly averages from 1974 to 2003 and the number of cholera outbreaks in Iran from 1974 to 2005 (red; as in Emch et al. (2008)). (B) A simulation with model (2) under seasonal forcing (see Eq. 4) and $R_0 = 1.2$, $\epsilon = 0.7143$, $Q_0 = 0.02\ days^{-1}$, $\lambda = 0.02\ days^{-1}$; $\rho = 0.00055\ day^{-1}$; other parameters as in Bertuzzo et al. (2008): $\mu = 0.00005\ days^{-1}$, $\beta = 1\ days^{-1}$, $\gamma = 0.2\ days^{-1}$, $\alpha = 0\ days^{-1}$, $\mu_B = 0.228\ days^{-1}$. (For interpretation of the references to colour in this figure legend, the reader is referred to the web version of the article.)

assume in this case $R_0 = 1.2$), the model exhibits a periodic behavior, with one yearly peak of cholera prevalence. The maximum number of outbreaks in Iran occurs three or four months after the lowest rainfall, which corresponds to the minimum bacterial dilution (Fig. 2A). Interestingly, the model reproduces correctly a similar time lag between the two patterns (Fig. 2B). Delays of the same kind have been observed also in other regions, such as Central Amazonia (Pascual et al., 2002; Codeco, 2001). We obtain such patterns for a reasonable value of the retention time of the water reservoir, equal to 50 days. This parameter is prominent in determining how much the minimum water level should lag with respect to the minimum water input, because it sets the response time of water reservoir volume with respect to the input. The delay between the minimum water volume and the epidemiological peak is then set by the basic reproductive number R_0, as it determines the threshold on susceptible population for the epidemic to occur.

Other hydrological regimes, not displaying a single rain period per year, are worth being considered, to investigate whether the resulting epidemiological patterns can be mimicked by our model. Some studies (Pascual et al., 2002; Altizer et al., 2006; Ruiz-Moreno et al., 2007) point out that bimodal rainfall patterns throughout the year can cause dramatic changes in the epidemiological patterns. In the 'wet' regions of the Indian districts of Madras Presidency (the Administrative subdivision for British colonies), where two rain seasons are present (one around May, the other in October), cholera appears quite regularly every year. On the contrary, in Madras regions, where one rainfall peak per year is registered, disease outbreaks are recurrent but with irregular frequencies and amplitude.

We run our model by taking as water input the actual monthly averages of rainfall shown in Ruiz-Moreno et al. (2007) for the wet province of Trichinopoly (India), normalizing the quantities shown there so that:

$$Q(t) = Q_0 \frac{r_{Tr}(t)}{\max r_{Tr}(t)} \tag{5}$$

where $r_{Tr}(t)$ is the monthly averaged rainfall pattern as reported in Ruiz-Moreno et al. (2007).

Fig. 3 shows $r_{Tr}(t)$ (blue dotted line) and cholera normalized prevalence $I_{Tr}(t)$ (yellow dashed line), also derived from data on cholera mortality shown in Ruiz-Moreno et al. (2007) as a proxy. We then compare the latter to the long-term simulation (black solid curve) of our model (2), when forced assuming that the water input pattern follows each year the rainfall pattern depicted in Fig. 3. Daily prevalences obtained from the model have been aggregated to monthly values and normalized. Note that, if the rainfall input repeated every year in the same way as in our case, the simulated asymptotic pattern would be periodic. This allows us to ascribe the

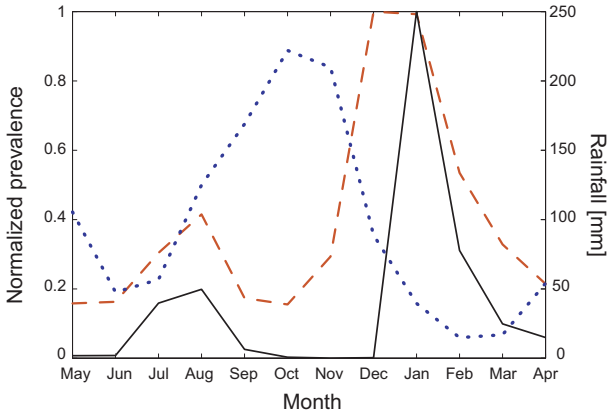

Fig. 3. Comparison between data on monthly averages for cholera insurgence (yellow dashed line) and rainfall (blue dotted line) for the province of Trichinopoly, as shown in Ruiz-Moreno et al. (2007), and a model simulation (black solid line) with $R_0 = 7.5$, $\lambda = 0.2\ day^{-1}$; $\rho = 0.00055\ day^{-1}$ and water input given by equation (3); other parameters as in Bertuzzo et al. (2008): $\mu = 0.00005\ days^{-1}$, $\beta = 1\ days^{-1}$, $\gamma = 0.2\ days^{-1}$, $\alpha = 0\ days^{-1}$, $\mu_B = 0.228\ days^{-1}$. (For interpretation of the references to colour in this figure legend, the reader is referred to the web version of the article.)

dynamics shown in Fig. 3 to the intrinsic dynamics of the model, which proves quite effective in grasping the overall mechanics of disease insurgence. In fact the winter peak occurs in January, when rainfall is decreasing, but before the rainfall minimum. The epidemiological peak drains the Susceptible basin; so, when conditions for disease outbreak (i.e., high vibrio concentration) occur again, near the second rainfall minimum (in June), the subsequent spring peak of cholera prevalence is approximately 60% lower. This result highlights the non-triviality of the interplay between human compartments, concentration of *V. cholerae* and the fluctuations of the water reservoir, as no unique relationship between the water input timing and the timing of the epidemic can be identified.

Data on long-term dynamics of cholera insurgence show high variations in the magnitude of prevalence peaks (King et al., 2008; Koelle et al., 2005; Ruiz-Moreno et al., 2007; de Magny et al., 2008; Glass et al., 1982; Huq et al., 2005; Islam et al., 2009; Pascual et al., 2008). Some studies have explicitly highlighted the large unpredictability of prevalence peaks (Pascual et al., 2002; Altizer et al., 2006). This might lead to the conclusion that a chaotic behavior can be characteristic of long-term cholera patterns.

Bifurcation analysis of the model

To understand the full complexity of seasonal epidemiological patterns, it is helpful to conduct a systematic analysis of the

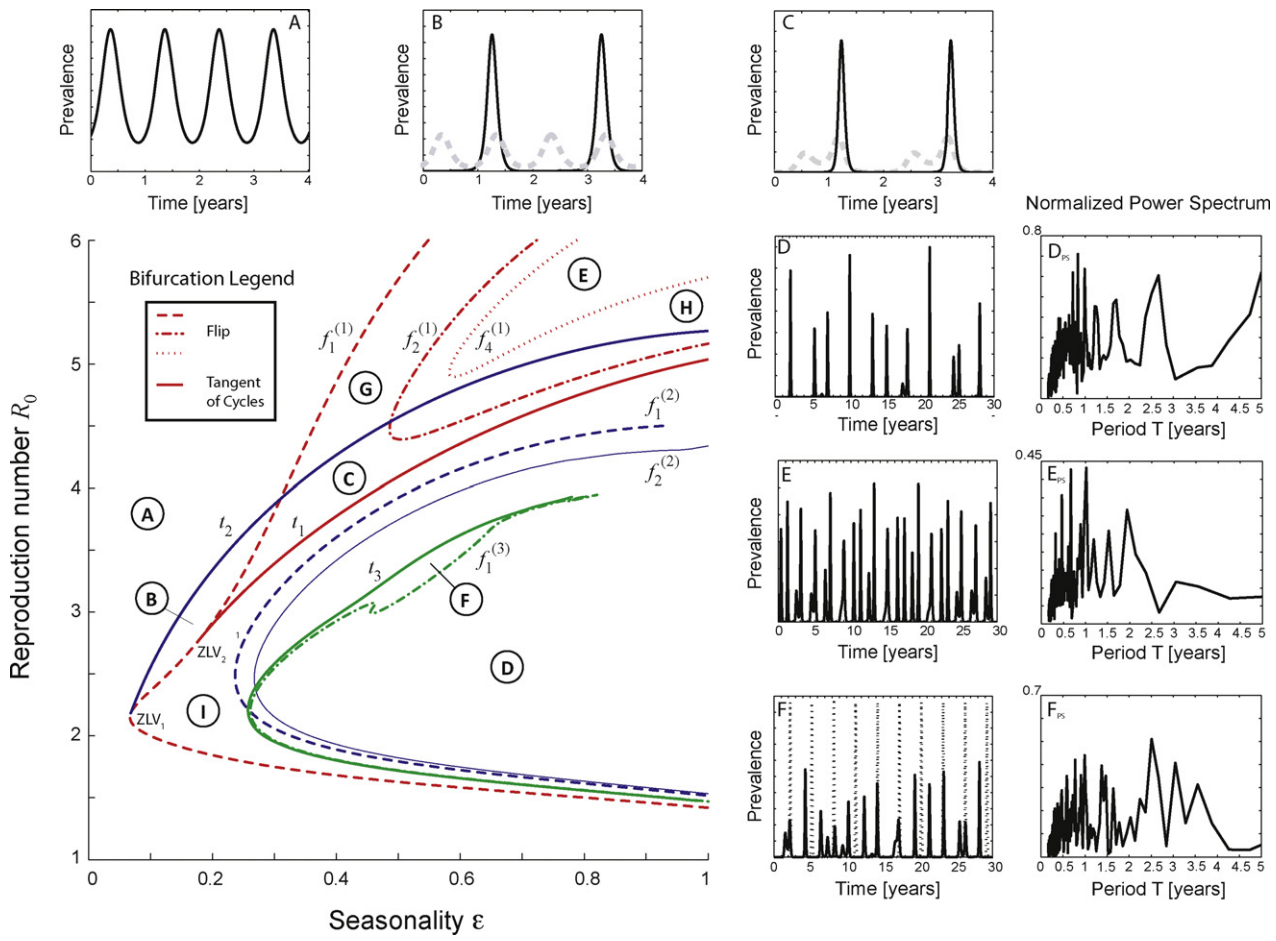

Fig. 4. Bifurcation diagram of model (2) in the parameter space (ϵ, R_0 for $\lambda = Q_0 = 0.01\ days^{-1}$. Line types and symbols explained in the Appendix A. Unspecified parameters as in Fig. 2.

qualitative long-term behaviors of our model. The most effective way of cataloguing the functioning modes of nonlinear systems such as (2) is bifurcation analysis (Kuznetsov, 1995). By using software that implements continuation techniques (e.g. AUTO or MATCONT; Dhooge et al., 2003), it is possible to compute in relevant parameter spaces the bifurcation surfaces partitioning parametric regions where the model phase portraits are topologically equivalent. For example, parametric conditions for which the model exhibits one attracting limit cycle of period 1 year are separated by a surface from those where one single cycle of period 2 or a chaotic attractor emerges.

This kind of analysis is especially suited to the case at hand, because, as explained in the Introduction, uncertainties and variations are mainly limited to three parameters, two characterizing the hydrological regime (λ, ϵ) and one the epidemiological process (R_0). In particular, the amplitude of the forcing or degree of seasonality ϵ is representative of the climatic regime of a region and can widely vary throughout the world, while the basic reproductive number of the disease R_0 is very seldom estimated in the cholera literature. The retention time of the water reservoir is also an important uncertainty factor when describing the hydrological dynamics and thus governs the interactions between environment and vibrio concentration: for this reason the robustness of the analysis with respect to this parameter will be tested. Fig. 4 shows the bifurcation diagram of the model in the parameter space (ϵ, R_0), obtained for a reservoir characterized by a retention time of $1/\lambda = 100$ days, together with typical temporal patterns of the disease obtained by the model. Each panel shows an example of the prevalence fluctuations corresponding to a different parametric region. To the far right we also show the characteristic power spectra of the chaotic time series depicted aside.

Appendix A contains a detailed description of the structures depicted in the main bifurcation diagram (Fig. 4). We particularly underline the presence of regions in which there is bistability, namely the coexistence of periodic attractors of different characteristic period. Three main stable limit cycles, in fact, can be found indifferent regions of the parameter space under study, with a characteristic basic periodicity of 1, 2 and 3 years. The formation of the 2(3)-year cycle via a tangent of cycles bifurcation is marked by the blue(green) solid line, while the red solid line locates the disappearance of the 1-year cycle (For interpretation of the references to colour in this text, the reader is referred to the web version of the article.). In regions B and C, thus, bistability between the 1-year period – which, though, acquires biannual periodicity in region C – and the 2-year period attractors is encountered, whereas regions D and F show coexistence between the 2-year period and the 3-year period attractors. This is a feature that holds important epidemiological significance, as simple variations in the values of state variables – say, in the number of vibrios – can strongly influence the general epidemiological pattern, shifting the system trajectories to another attractor. The formation of bistability regions was also observed in other bifurcation diagrams of epidemiological models, chiefly in Kuznetsov and Piccardi (1994) and in Earn et al. (2000), for low-intermediate levels of the contact rate of the disease, which can be taken as a proxy of the basic reproductive number for comparison with our results. In fact, in our model too we find that bistability is to be expected for low or intermediate values of R_0.

At increasing values of the degree of seasonality ϵ, we also verify the appearance of chaotic behavior, which occurs as periodic attractors progressively double their characteristic period via what is called a Feigenbaum cascade of flip bifurcations – detailed with dashed, dashed-dotted and dotted lines in Fig. 4; colors refer to different attractors, as explained above. Two chaotic regions are found, originated by different periodic attractors. More specifically, in region E one may find chaotic patterns generated by the limit cycle of annual period, while in region D there exists bistability between the chaotic attractors generated by the biannual and the triannual limit cycles. The trajectories arising from such parametric conditions show non-trivial signatures, as shown in the far right panels D_{PS}, E_{PS} and F_{PS} of Fig. 4. There we show the normalized values of the Fast Fourier Transform (FFT) spectra of suitably long windows of model simulations of cholera incidence (aggregated on a monthly basis), for values of the parameters corresponding to the respective areas of the bifurcation diagram. The characteristic periodicity of the cycle from which each chaotic attractor was generated leaves its fingerprint, as one can detect spikes located at 1-year (E_{PS}), 2-year (F_{PS}) and 3-year (D_{PS}) periodicities. Interestingly, however, many other frequencies, greatly attenuated when trajectories are simply periodic, emerge as important from the spectral analysis of chaotic patterns. Biannual frequencies arise where a 1-year periodicity is preponderant (panel E_{PS}), while annual frequencies emerge when 2-year and 3-year peaks explain much of the fluctuations of incidence trajectories (panels D_{PS} and F_{PS}).

A comparison with the dominant frequencies of real long-term time series of cholera incidence can be useful to determine the significance of the above results. We have taken weekly epidemiological reports on cholera cases, reported by WHO, and aggregated them on a monthly basis (distributing cases between months accordingly). We assume that no reports for a particular nation and month correspond to zero cases. In Fig. 5 we show, again, the normalized values of the FFT spectra of the time series of new cholera cases in three countries, that we choose for their long and mostly complete records (approximately 35 years for Cameroon and Niger, 20 for the Philippines). Spectral analysis is restricted to 5 years' periods, as a significant analysis of lower frequencies would require longer time series. Moreover, lower frequencies can be controlled by interannual variation of climatic variable (e.g. ENSO for the pacific regions (Pascual et al., 2000; Rodo et al., 2002)). Our model does not account for interannual forcings and thus it cannot consistently capture frequencies lower than 5 years of period. Despite these shortcomings, we find important similarities between the spectra we obtained from chaotic model trajectories and the ones depicted in Fig. 5, not only qualitatively, but also quantitatively. Cameroon and Niger show, in fact, strong biannual and triannual periodicities respectively, which closely match the ones characteristic of chaotic patterns in region D of Fig. 4 (see panels F_{PS} and D_{PS}). Along with the main periodic component, both data and model show many other excited frequencies, of intra-annual, annual and multi-annual periodicities. More specifically, Niger FFT spectrum shows important biannual and annual components, which can be also observed in panel D_{PS} of Fig. 4. Similarly, Cameroon epidemiological pattern is characterized by a set of different periodicities, not only involving the biannual main component, but also significant frequencies of lesser – 1 year and less – and greater – 3 years and

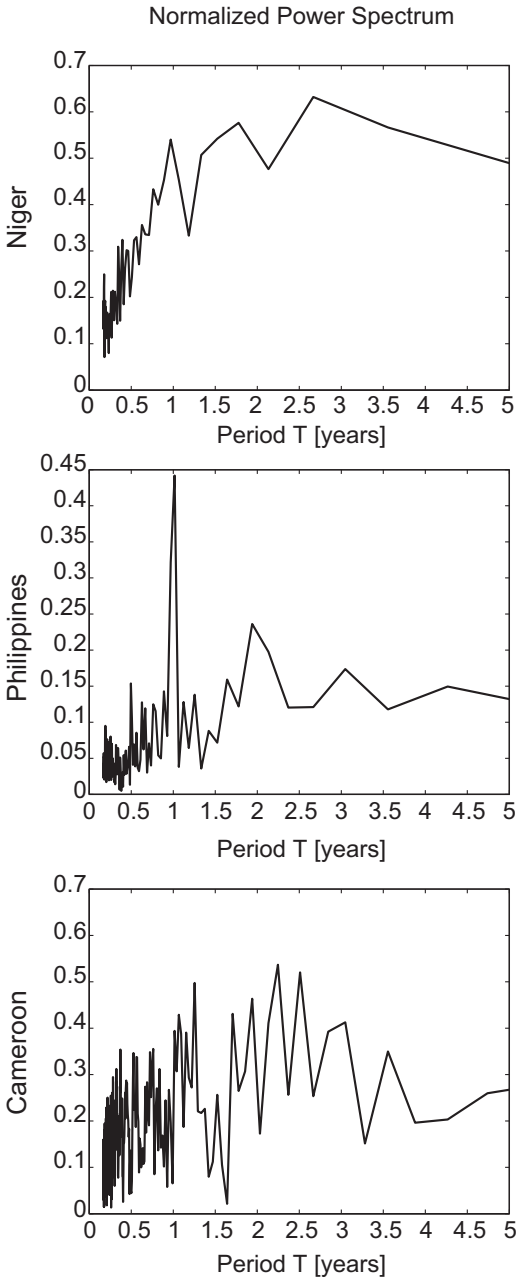

Fig. 5. Normalized power spectra of monthly aggregated weekly epidemiological reports (WHO) for Niger, Philippines and Cameroon.

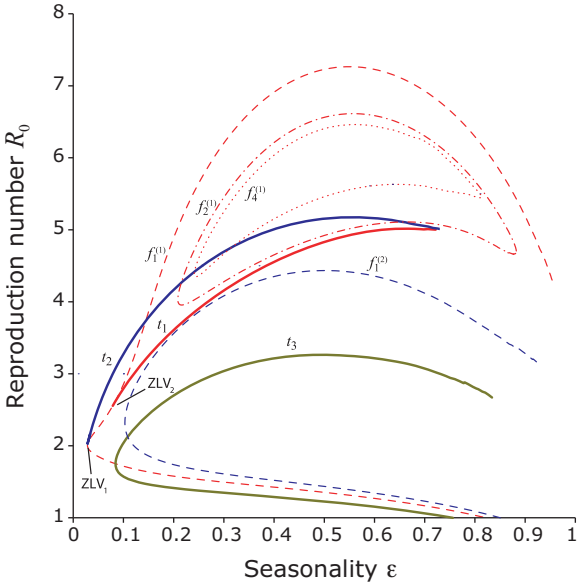

Fig. 6. As Fig. 4, but for $\lambda = Q_0 = 0.1\ \text{day}^{-1}$.

more – period. This pattern is also caught by the spectrum of the chaotic trajectories of the biannual attractor, as seen in panel F_{PS} of Fig. 4. The Philippines, instead, are characterized by an important annual component, with a much lower peak at the 2-year periodicity, a pattern also emerging from the chaotic trajectories of region E of Fig. 4 (see panel E_{PS}).

One might wonder whether adding random noise – e.g. a log-normal factor to water input, to simulate rainfall daily variability – to models with parameters corresponding to nonchaotic patterns would lead to more realistic spectra. The answer is negative, as it emerges from our simulations: there would be only slight variations in high frequency components, as expected. Therefore, it looks like the broad and diversified spectra of actual time series can only be obtained with parameters corresponding to chaotic patterns, and not simply by adding noise to more regular patterns.

These findings raise the question of whether the difference between endemic regions, where cholera appears every year (the Philippines, for instance), and epidemic regions (Cameroon and Niger), where outbreaks are sparsely distributed along the years (Sack et al., 2003; Ruiz-Moreno et al., 2007) may well be simply ascribed to different values of R_0, which cause outbreaks characterized by different frequencies. It is also worth noting that, compared to airborne diseases, such as measles (Kuznetsov and Piccardi, 1994) or influenza (Casagrandi et al., 2006), environmental drivers of waterborne diseases such as cholera can display a

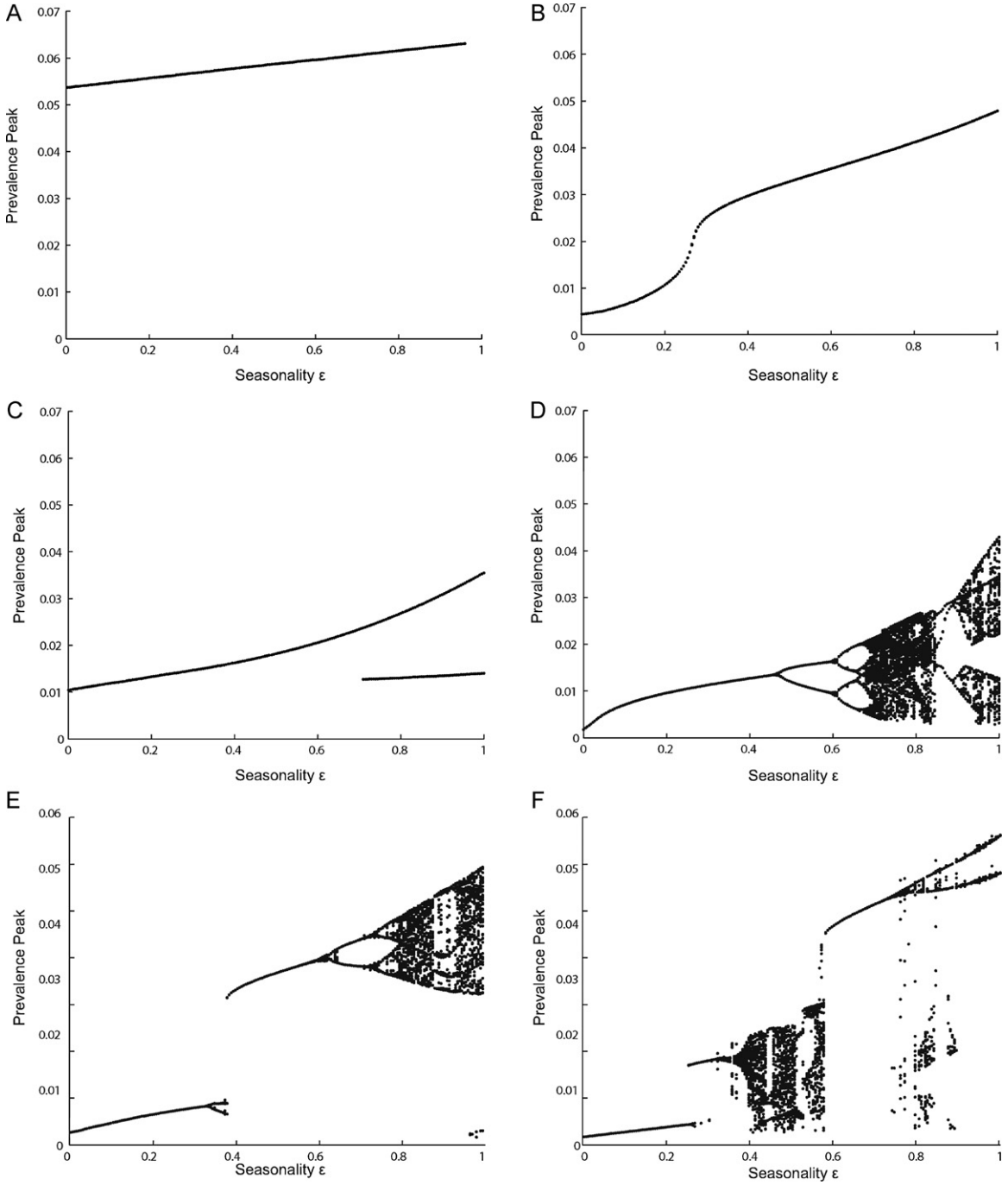

Fig. 7. Feigenbaum diagrams for varying values of loss of immunity rate: $1/\rho = 12$ weeks (A.); 1 year (B.); 3 years (C.); 5 years (D.); 8 years (E.); 10 years (F.). $R_0 = 5.5$ and $\lambda = Q_0 = 0.01\ days^{-1}$. Unspecified parameters as in Fig. 2.

seasonality degree ϵ as high as 80% or more. In fact, we expect the values of ϵ in historically endemic regions, where monsoonal regimes prevail, to be typically high, as water input is definitely concentrated in specific periods of time during the year. According to the model outcomes, we should therefore expect, in general, complex epidemiological patterns of the disease.

To verify the robustness of this global picture of our model behaviors we also analyze the bifurcation diagram for a different value of the water retention time λ^{-1}, which is the third parameter that can widely vary in different situations. We choose, in particular, to increase the value of λ to 0.1 day^{-1}, thus shortening the average water retention time to 10 days. The previous value (0.01 day^{-1}), in fact, identifies reservoirs with residence time of approximately 3 months, which can refer to water provisioning from and disposal to, say, a small lake. In Fig. 6 we instead consider the opposite extreme of very small ponds, which get inundated or refilled by rainfall, but are rapidly drained, thus causing much faster hydro-epidemiological dynamics in the system. This new parameter setting leads to a slightly more complicated diagram, as shown in Fig. 6. In fact, for a fixed value of R_0, the sequence of period doubling bifurcations leading to a region of chaotic patterns occurs for smaller ϵ's, compared to Fig. 4. For instance, chaos is possible with $\epsilon = 0.2$ and $R_0 = 2$, whereas these parameters corresponded to a 2-year cycle in the system with $\lambda = 0.01$ days^{-1}.

At the same time, the robustness of the previous analysis is confirmed by observing that the basic topological structure of the bifurcation diagram is respected: one can still find the bistability region (again, between the blue and the red solid lines) and the two chaos regions, for different values of R_0. The upper chaotic region is closed and restricted by the seasonality range $0.25 < \epsilon < 0.85$. Higher or lower values of the forcing amplitude will lead to periodic dynamics, with return time of one year. Important differences arise, however, from an epidemiological viewpoint, between period 1 cycles at low and high values of ϵ. We find, for instance, that the peak prevalence for $\epsilon = 0.1$ is 0.0129, while we obtain a value of 0.065 for $\epsilon = 0.9$, at $R_0 = 6$. Moreover, the tangent bifurcation of period three cycles (t_3 curve) is again observed.

Another parameter whose value has been recently questioned is the duration of immunity after recovery from cholera infection. Even if the great majority of immunological studies and modeling exercises indicate that immunity should last between 3 and 10 years, King et al. (2008) reconstructed from cholera incidence time series a short-term immunity of only 12 weeks. To compare the behavior of the model for different values of the rate of loss of immunity, we show in Fig. 7 the results pertaining four different values of immunity duration, namely 12 weeks, 1 year, 3 years and 5 years. The analysis here shown is a so-called Feigenbaum diagram, displaying the values of cholera prevalence peaks as a function of the degree of seasonality ϵ, for a fixed basic reproductive number $R_0 = 5.5$. Results prove to be consistent with these also for $R_0 = 2.5$ (not shown). Panels (A)–(C), corresponding to the shorter durations of immunity, do not show any complexity arising. Apart from an increasing amplitude of the prevalence peaks, driven by the more pronounced seasonal oscillations of water input, the annual periodic pattern is qualitatively maintained, except for a flip bifurcation emerging in diagram (B), corresponding to $1/\rho = 1$ year, which does not affect the general annual periodicity of such pattern. Chaotic patterns only appear in the diagram related to the longest immunity period, coherently with what we obtained in Fig. 4. The difference is explained by the fact that the faster the loss of immunity is, the more a SIRS-based model like the one we presented resembles a simple SIS model, with practically no role of the R class. This induces faster replenishment dynamics of the Susceptible compartment and a simple synchronization of epidemiological dynamics with the external forcing.

Conclusions

We have proposed a new model to study cholera dynamics, which explicitly takes into account temporal fluctuations of the water volume hosting the pathogen *V. cholerae*. To this end, we have added two compartments to the standard SIB model for cholera, originally proposed by Codeco (2001): the recovered compartment R, which is important to understand the long term dynamics of the disease, and the hydrologic fluctuations of the water volume W available to a certain human community. In order to mimic the processes of dilution that control bacterial concentrations in the system, the input (rainfall or runoff) to W, which varies over time following a simple (and regular) seasonal pattern, is periodically forced. We have shown that, even with this simple description of hydrological phenomena, the model can reproduce the epidemiological courses that characterize the periodic insurgence of the disease in various areas of the world. In particular, the model can quantitatively describe the delay between drought seasons – during which there is a high vibrio concentration in the water – and prevalence peaks. This has been observed in countries where cholera has been present for decades (e.g. Iran). We have also investigated the effect of bimodal forcings which better describe the yearly rainfall patterns of other geographical regions (e.g. India). If forced with the actual values of water input that are observed for endemic regions in the province of Madras, India, the model is able to quite well reproduce the recorded patterns of seasonal cholera which, in this particular case, occurs twice per year. Not only the timing, but also the relative amplitude of peaks is in fact quite satisfactorily reproduced. Finally, we have analyzed the whole range of model behaviors in the parameter space of the degree of seasonality ϵ and of the basic reproduction number R_0, which we choose as most significant and subject to wider variations (other parameters are assumed from the relevant literature or from available data). Bifurcation analysis revealed the presence of behaviors also found in real data, including non-periodic, chaotic dynamics. We observed an increased complexity of model behaviors for intermediate or high values of ϵ coherently with previous results Kuznetsov and Piccardi (1994). Also, we have found two distinct parameter regions where different chaotic attractors emerge, which however display different average epidemic frequencies (which increase with R_0). Power spectra referring to chaotic trajectories show significant similarities with real data time series in both endemic and epidemic countries. We thus hypothesize that the difference between endemic and epidemic regions might be different intensities of the disease, as expressed by different basic reproductive numbers. Moreover, different values of the loss of immunity rate show that only a relatively long time of immunity can induce complex dynamics in the system.

Despite the ability of such a simple model to describe many actual temporal patterns of cholera, there exist some cases that cannot be explained by the dilution mechanism only. Patterns, such as those typically observed for certain Bangladesh regions (Matlab in particular; see e.g. Emch et al., 2010), display two outbursts per year - one between April and May (spring peak), the other around October/November (autumn peak), even if there is only one rainfall peak per year. We speculate, though, that this peculiarity might be due to the concurrence of two mechanisms: (a) the disruption of sanitation systems during floods or hyper-supply of pathogens, which counter the dilution effect, and (b) spatially explicit dynamics, which we do not consider here but that are accounted for in several studies (see e.g. Bouma and Pascual, 2001).

As the recent Haiti epidemics testifies, the development of analytical tools that can help not only to predict but also to understand the basic processes underlying the intertwinement between environmental variability and the insurgence of cholera is much needed. Models including both the epidemiological compartments

and the environmental matrix in which the disease unfolds can greatly help in setting up intervention policies and emergency management alternatives. Making them space and time-specific can strengthen their effectiveness and reliability. Needless to say, such effort is most effective when supported by consistent data surveys, which can help in detailing the environmental and epidemiological characteristics of the area hit by the disease outbreaks.

Acknowledgments

L.R., E.B., L.M. and A.R. gratefully acknowledge the support provided by ERC advanced grant program through the project *RINEC*-227612. Funds provided by Fond National Suisse de la Recherche Scientifique Grant 200021_124930 are gratefully acknowledged. I.R.-I. acknowledges the support of the James S.McDonnell Foundation through a grant for Studying Complex Systems (220020138). MG acknowledges the support from the SFN/FNS project IZK0Z2 139537/1 for international cooperation.

Appendix A.

We detail here the structure of the bifurcation diagram shown in Fig. 4. At small ϵ's (region A), the system exhibits a stable one-year cycle. By varying the parameter values, such periodic attractor loses stability in favor of other attractors that undergo a series of bifurcations all depicted as red curves in Fig. 4. The dashed red curve $f_1^{(1)}$ is a flip bifurcation which is subcritical within the interval (ZLV_1, ZLV_2) and supercritical elsewhere. Crossing the supercritical part of $f_1^{(1)}$ from left to right (regions G and I) causes the one-year cycle attractor to lose its stability in favor of a cycle with a 2-year period. From an epidemiological viewpoint, it is important to emphasize that the period doubling does not reflect an actual temporal displacement of prevalence peaks but a differentiation in their amplitude. In other words, close to the right of the supercritical part of $f_1^{(1)}$, there is a periodic attractor whose prevalence peaks every year, but with two slightly different peaks in odd and even years. The red dashed and dotted line $f_2^{(1)}$ is a supercritical flip bifurcation of the 2-year cycle just described. Inside the convex parametric region H formed by the curve (and close to it) a 4-year period cycle is stable. This 4-year cycle also loses its stability via period doubling at the red dotted flip bifurcation curve $f_4^{(1)}$. A cascade of flip bifurcations (Feigenbaum cascade) occurs nearby $f_4^{(1)}$ and a parametric region where model (2) shows chaotic behavior is entered (region E). The corresponding temporal patterns shown in panel 4E are indeed very resemblant to actual long-term time-series (as extensively discussed above). While the amplitude and the timing of each peak is unpredictable for the chaotic attractors in this parametric region, the average return time of two prevalence peaks (i.e., of cholera outbreaks) remains rather close to approximately one year, yet decreases with increasing R_0.

The solid red curve t_1 is a tangent of cycles bifurcation that involves the 2-year periodic attractor originated at the flip bifurcation $f_1^{(1)}$ and another unstable period 2 cycle. At t_1, these two cycles collide and disappear for parametric values at the right of it (region I).

There is a second important structure, depicted with blue curves, in the bifurcation diagram of Fig. 4. The blue solid line t_2 is a tangent bifurcation of cycles that identifies the formation of an attractor of period 2 years *sensu stricto*. In other words, this cycle has an epidemiological periodicity of 2 years, i.e. it has prevalence peaks that only appear every 2 years (solid time-series in Fig. 4 panel B). The parametric region between the solid blue and red curves is therefore characterized by bistability, namely the system can alternatively converge to one cyclic solution of period 2 or another of either period 1 (region B) or 2 (with an interpeak period of 1 year though, region C). The period 2 attractor emerged at t_2 also undergoes a cascade of flip bifurcations. The blue dashed curve $f_1^{(2)}$ and the dashed and dotted $f_2^{(2)}$ curve are the first two flip bifurcations of a sequence leading to a region (labeled as D) where the system displays chaotic behavior. As noticed for the strange attractors of region E, chaotic regimes obtained in region D also maintain to some extent the characteristic periodicity of the original cycle that underwent the Feigenbaum cascade. The mean return time of aperiodic patterns in region D ranges from values around 2.36 years for $R_0 = 3$, to values of nearly 1.64 years for $R_0 = 4$.

Within the chaotic region D, other interesting structures emerge, although it is difficult to continue the bifurcations, for numerical reasons. As an example, we show a tangent bifurcation of period three cycles (solid green curve, t_3) and a supercritical flip bifurcation ($f_1^{(3)}$), where the period three cyclic attractor originated at t_3 doubles its period. In region F we therefore find bistability, which implies the coexistence of a chaotic attractor and a stable period 3 cycle (see panel F).

References

Akanda, A.S., Jutla, S., Islam, S., 2009. Dual peak cholera transmission in Bengal delta: a hydroclimatological explanation. Geophysical Research Letters 36, L19401.
Altizer, S., Dobson, A., Hosseini, P., Hudson, P., Pascual, M., Rohani, P., 2006. Seasonality and the dynamics of infectious diseases. Ecology Letters 9, 467–484.
Anderson, R., May, R., 1992. Infectious Diseases of Humans. Oxford University Press, Oxford, UK.
Bertuzzo, E., Azaele, S., Maritan, A., Gatto, M., Rodriguez-Iturbe, I., Rinaldo, A., 2008. On the space-time evolution of a cholera epidemic. Water Resources Research 44, W01424.
Bertuzzo, E., Casagrandi, R., Gatto, M., Rodriguez-Iturbe, I., Rinaldo, A., 2010. On spatially explicit models of cholera epidemics. Journal of the Royal Society Interface 7, 321–333.
Bertuzzo, E., Mari, L., Righetto, L., Gatto, M., Casagrandi, R., Blokesch, M., Rodriguez-Iturbe, I., Rinaldo, A., 2011. Prediction of the spatial evolution and effects of control measures for the unfolding Haiti cholera outbreak. Geophysical Research Letters 38.
Bouma, M., Pascual, M., 2001. Seasonal and interannual cycles of endemic cholera in Bengal 1891–1940 in relation to climate and geography. Hydrobiologia 460, 147–156.
Brutsaert, W., 2005. Hydrology: An Introduction. Cambridge University Press.
Casagrandi, R., Bolzoni, L., Levin, S., Andreasen, V., 2006. The SIRC model and influenza A. Mathematical Biosciences 200, 152–169.
Chao, D.L., Halloran, M.E., Longini Jr., I.M., 2011. Vaccination strategies for epidemic cholera in Haiti with implications for the developing world. Proceedings of the National Academy of Sciences of the United States of America 108, 7081–7085.
Clemens, J.D., Sack, D.A., Harris, J.R., van Loon, F., Chakrabortya, J., Ahmed, F., Rao, M.R., Khan, M.R., Yunus, M., Huda, N., Stanton, B.F., Kay, B., Eeckels, R., Sack, D.A., Walter, S., Svennerholm, A.M., Holmgren, J., 1990. Field trial of oral cholera vaccines in Bangladesh: results from three-year follow-up. Lancet 335, 270–273.
Codeco, C., 2001. Endemic and epidemic dynamics of cholera: the role of the aquatic reservoir, BMC Infectious Diseases 1.
Colwell, R., 1996. Global climate and infectious disease: the cholera paradigm. Science 274, 2025–2031.
de Magny, G.C., Murtugudde, R., Sapiano, M.R.P., Nizam, A., Brown, C.W., Busalacchi, A.J., Yunus, M., Nair, G.B., Gil, A.I., Lanata, C.F., Calkins, J., Manna, B., Rajendran, K., Bhattacharya, M.K., Huq, A., Sack, R.B., Colwell, R.R., 2008. Environmental signatures associated with cholera epidemics. Proceedings of the National Academy of Sciences of the United States of America 105, 17676–17681.
Dhooge, A., Govaerts, W., Kuznetsov, Y., 2003. MATCONT: a MATLAB package for numerical bifurcation analysis of ODEs. ACM Transactions on Mathematical Software 29, 141–164.
Earn, D., Rohani, P., Bolker, B., Grenfell, B., 2000. A simple model for complex dynamical transitions in epidemics. Science 287, 667–670.
Emch, M., Feldacker, C., Islam, M.S., Ali, M., 2008. Seasonality of cholera from 1974 to 2005: a review of global patterns. International Journal of Health Geographics 7, 31.
Emch, M., Yunus, M., Escamilla, V., Feldacker, C., Ali, M., 2010. Local population and regional environmental drivers of cholera in Bangladesh. Environmental Health 9.
Glass, R., Becker, S., Huq, M., Stoll, B., Khan, M., Merson, M., Lee, J., Black, R., 1982. Endemic cholera in rural Bangladesh, 1966–1980. American Journal of Epidemiology 116, 959–970.
Hartley, D., Morris, J., Smith, D.L., 2006. Hyperinfectivity: a critical element in the ability of V. cholerae to cause epidemics? PLoS Medicine 3, 63–69.
Huq, A., Sack, R., Nizam, A., Longini, I., Nair, G., Ali, A., Morris, J., Khan, M., Siddique, A., Yunus, M., Albert, M., Sack, D., Colwell, R., 2005.

Critical factors influencing the occurrence of Vibrio cholerae in the environment of Bangladesh. Applied and Environmental Microbiology 71, 4645–4654.
Iran Meterological Service, 2011. Iran rainfall data are available online at http://www.irimo.ir/english/monthly&annual/map/index.asp.
Islam, M.S., Sharker, M.A.Y., Rheman, S., Hossain, S., Mahmud, Z.H., Islam, M.S., Uddin, A.M.K., Yunus, M., Osman, M.S., Ernst, R., Rector, I., Larson, C.P., Luby, S.P., Endtz, H.P., Cravioto, A., 2009. Effects of local climate variability on transmission dynamics of cholera in Matlab, Bangladesh. Transactions of the Royal Society of Tropical Medicine and Hygiene 103, 1165–1170.
King, A., Ionides, E., Pascual, M., Bouma, M., 2008. Inapparent infections and cholera dynamics. Nature 454, 877–880.
Koelle, K., Rodo, X., Pascual, M., Yunus, M., Mustafa, G., 2005. Refractory periods and climate forcing in cholera dynamics. Nature 436, 696–700.
Kuznetsov, Y., Piccardi, C., 1994. Bifurcation-analysis of periodic SEIR and SIR epidemic models. Journal of Mathematical Biology 32, 109–121.
Kuznetsov, Y., 1995. Elements of Applied Bifurcation Theory. Springer-Verlag, New York, USA.
Lipp, E., Huq, A., Colwell, R., 2002. Effects of global climate on infectious disease: the cholera model. Clinical Microbiology Reviews 15, 757.
Mari, L., Bertuzzo, E., Righetto, L., Casagrandi, R., Gatto, M., Rodriguez-Iturbe, I., Rinaldo, A., 2012. Modeling cholera epidemics: the role of human mobility and sanitation conditions. Journal of the Royal Society Interface 9, 376–388, doi:10.1098/rsif.2011.0304.
Neilan, R.L.M., Schaefer, E., Gaff, H., Fister, K.R., Lenhart, S., 2010. Modeling Optimal intervention strategies for cholera. Bulletin of Mathematical Biology 72, 2004–2018.
PAHO, 2010. EOC Situation Report # 17, Technical Report. Pan-American Health Organization, Regional Office of the World Health Organization. Online at http://new.paho.org/hq/images/Atlas_IHR/CholeraHispaniola/atlas.html.
Pascual, M., Rodo, X., Ellner, S., Colwell, R., Bouma, M., 2000. Cholera dynamics and El Nino-Southern oscillation. Science 289, 1766–1769.
Pascual, M., Bouma, M.J., Dobson, A.P., 2002. Cholera and climate: revisiting the quantitative evidence. Microbes and Infection 4, 237–245.
Pascual, M., Chaves, L.F., Cash, B., Rodó, X., Yunus, Md., 2008. Predicting endemic cholera: the role of climate variability and disease dynamics. Climate Research 36, 131–140.
Righetto, L., Bertuzzo, E., Casagrandi, R., Gatto, M., Rodriguez-Iturbe, I., Rinaldo, A., 2011. Modelling human movement in cholera spreading along fluvial systems. Ecohydrology 4, 49–55.
Rodo, X., Pascual, M., Fuchs, G., Faruque, A., 2002. ENSO and cholera: a nonstationary link related to climate change? Proceedings of the National Academy of Sciences of the United States of America 99, 12901–12906.
Ruiz-Moreno, D., Pascual, M., Bouma, M., Dobson, A., Cash, B., 2007. Cholera seasonality in Madras (1901–4940): dual role for rainfall in endemic and epidemic regions. Ecohealth 4, 52–62.
Sack, R., Siddique, A., Longini, I., Nizam, A., Yunus, M., Islam, M., Morris, J., Ali, A., Huq, A., Nair, G., Qadri, F., Faruque, S., Sack, D., Colwell, R., 2003. A 4-year study of the epidemiology of Vibrio cholerae in four rural areas of Bangladesh. Journal of Infectious Diseases 187, 96–101.
Tuite, A.R., Tien, J., Eisenberg, M., Earn, D., Ma, J., Fisman, N., 2011. Cholera epidemic in Haiti, 2010: using a transmission model to explain spatial spread of disease and identify optimal control interventions. Annals of Internal Medicine 154, 593–601, doi:10.1059/0003-4819-154-9-201105030-00334.